Kinetic Studies of the Unfolding-Refolding of Horse Muscle Phosphoglycerate Kinase Induced by Guanidine Hydrochloride†

J.-M. Betton, M. Desmadril, A. Mitraki, and J. M. Yon*
Laboratoire d'Enzymologie physico-chimique et moléculaire, Groupe de Recherche du Centre National de la Recherche Scientifique associé à l'Université de Paris-Sud, 91405 F-Orsay, France
Received December 7, 1984; Revised Manuscript Received March 18, 1985

ABSTRACT: The kinetics of the unfolding and refolding of horse muscle phosphoglycerate kinase were studied with three different signals: (1) fluorescence emission intensity at 336 nm (excitation at 292 nm), (2) ellipticity at 220 nm, and (3) enzyme activity. The results corroborate the conclusion on the existence of intermediates in the folding pathway obtained from equilibrium studies. Kinetic studies showed at least two phases of refolding, as revealed by fluorescence as well as by circular dichroism measurements. During the fast phase, an intermediate was formed with a fluorescence intensity higher than that of the native protein, but devoid of enzyme activity. The fluorescence emission spectrum of this intermediate was determined. Only the slow phase was detected for the unfolding process; it was not attributable to proline isomerization. Several models were assumed, and simulated kinetics derived from these models were compared with the experimental results. A plausible one accounting for most of the data is proposed.

For small proteins, the unfolding and refolding transition under equilibrium conditions is generally a very cooperative process that can be described by a two-state approximation, intermediates when they do exist being insufficiently populated. Only kinetic studies are really decisive in establishing the occurrence of several steps along the folding pathway.

However, deviations from a two-state behavior have been observed in several cases, even under equilibrium conditions (1) either by the existence of an intermediate shoulder or plateau (2) or by noncoincidence of the transition curves observed from different signals (3) or by differences in ΔH obtained from van't Hoff plots and from calorimetric measurements. Relevant studies have been reviewed and discussed in Kim & Baldwin (1982) and Ghélis & Yon (1982). Stable intermediates at equilibrium generally occur for larger proteins folded in several domains.

In a previous study (Betton et al., 1984), the conformational transition of horse muscle phosphoglycerate kinase (PGK,[1] EC 2.7.2.3) was investigated under equilibrium conditions. The protein made up of two structural domains has been described as a "hinge-bending enzyme" (Banks et al., 1979; Blake & Rice, 1981). The unfolding-folding transition induced by Gdn-HCl was followed by four different signals: (1) enzyme activity; (2) variations in fluorescence emission intensity at 336 nm (excitation at 292 nm); (3) variations in absorbance at 286 and 292 nm; (4) variations in ellipticity at 220 nm. From (1) the noncoincidence of the different transition curves, (2) the asymmetry of the curve obtained from circular dichroism, and (3) thermodynamic analysis, we concluded to the occurrence of intermediates. Moreover, the data were found compatible with an independent refolding of each domain but with different equilibrium constants, the most favorable one referring to the refolding of the C-terminal domain.

Kinetics studies have been successfully applied to the detection of intermediates in the folding process of monomeric (Baldwin, 1975; Schmid, 1983) as well as oligomeric proteins (Rudolf et al., 1979; Jaenicke, 1981). In the present work, we studied the kinetics of the unfolding and refolding processes, using fluorescence, circular dichroism, and, in several experiments, enzyme activity to follow the transition.

Materials and Methods

Enzyme Preparation. Horse muscle PGK was prepared by the procedure of Scopes (1969) slightly modified by Blake (1972) as previously described (Desmadril et al., 1984; Betton et al., 1984).

Enzyme Assay. Standard assays were run according to the procedure of Bücher (1955) under the following conditions: 200 mM PIPES-50 mM K_2HPO_4 buffer, pH 7.5, containing 5 mM NH_4Cl, 10 mM mercaptoethanol, 500 μM NAD^+, 1 mM ADP, 20 mM $MgCl_2$, 500 μM glyceraldehyde 3-phosphate (GA3P), and 500 μM glyceraldehyde-3-phosphate dehydrogenase. NADH absorbance changes were recorded on a Cary 219 spectrophotometer equipped with a thermostated cell; temperature was 23 °C. The reaction was initiated by the addition of 10 μL of PGK solution to 1 mL of assay solution.

Materials. NAD^+, glyceraldehyde 3-phosphate, ADP, and coupling enzymes were from Sigma. GA3P was prepared from the diacetal barium salt following the instructions of the supplier. Solutions of Gdn-HCl (ultrapure product from Pierce) were prepared daily and their concentrations determined by refractometry (Nozaki, 1970).

Kinetics of Unfolding and Refolding. All experiments were performed in a 100 mM phosphate buffer, pH 7.5, containing 1 mM EDTA and 0.5 mM DTT at 23 °C. Different signals were used to follow the folding and refolding processes: fluorescence intensity at 336 nm (excitation at 292 nm), ellipticity at 220 nm, and enzyme activity.

Kinetics Followed by Fluorescence and Circular Dichroism. Native PGK (final concentration 2 μM) was added at zero

† This work has been sponsored by Centre National de la Recherche Scientifique (Groupe de Recherche 13 and A.T.P. 06931), Fondation pour la Recherche Médicale Française and Ministère de la Recherche et de la Technologie (Grant 81 E 1207), and NATO (Grant 0212 in collaboration with Professor M. Karplus from Harvard University).

[1] Abbreviations: ADP, adenosine 5′-diphosphate; ATP, adenosine 5′-triphosphate; DTT, DL-dithiothreitol; EDTA, ethylenediaminetetraacetic acid; GA3P, glyceraldehyde 3-phosphate; Gdn-HCl, guanidine hydrochloride; GPDH, glyceraldehyde-3-phosphate dehydrogenase; NAD^+, nicotinamide adenine dinucleotide; NADH, reduced nicotinamide adenine dinucleotide; PGK, 3-phosphoglycerate kinase; PIPES, 1,4-piperazinediethanesulfonic acid.

0006-2960/85/0424-4570$01.50/0

time to a solution containing Gdn-HCl (final concentration varying from 0.4 to 3 M). For renaturation kinetics, PGK previously denatured for 24 h in 6 M Gdn-HCl was added to zero time in the renaturation mixtures (final concentration of denaturant varying from 3 to 0.03 M Gdn-HCl). Unfolding as well as refolding kinetics were followed until the equilibrium was reached.

Fluorescence signal was followed on a Perkin-Elmer MPF 44B spectrofluorometer and ellipticity with an Autodichrograph MARK V (Jobin et Yvon). All kinetics were analyzed by a multilinear regression programm according to Cleland (1967), adapted to a Wang 2200 or Hewlett-Packard 9816 calculator, taking into account either one or two exponential terms.

Several experiments were performed with a Durrum D110 stopped-flow apparatus, measuring fluorescence emission through a MTO A340b filter. Syringes containing either PGK (5 μM) or Gdn-HCl solutions or standard buffer and the mixing chamber were thermostated at 23 °C. The signal recorded on an oscilloscope was stored on a magnetic band and later analyzed according to a multilinear program (through the courtesy of Dr. Gingold, Saclay) by an iterative search of the parameters with a Hewlett-Packard 9825 A calculator.

Kinetics Followed by Measuring the Enzyme Activity. The kinetics of unfolding and refolding were measured with 0.1 and 0.27 μM PGK in the denaturation or regeneration mixtures and 1 or 3 nM final concentration in the cell for activity measurements. The kinetics of unfolding were performed as follows: the protein previously incubated during different periods in the denaturant was added to the thermostated cell containing the mixture for measurements of the enzyme activity (23 °C). Under our experimental conditions, the rate of reactivation was much smaller than the rate of the enzyme reaction and did not interfere with these measurements.

Refolding kinetics were performed stepwise for Gdn-HCl concentrations smaller than 1 M where the initial activity was not null; PGK was previously denatured for 24 h in 6 M Gdn-HCl and then renatured for different times either in intermediate concentrations of Gdn-HCl or in the regeneration mixture.

Double-jump experiments, as reported by Brandts et al. (1975), were carried out to detect possible equilibrium between several denatured forms. A solution of 1 μM PGK was denatured in Gdn-HCl; aliquots were withdrawn at different times and directly introduced in the assay mixture. Under these conditions, the recovery of the enzyme activity showed a lag followed by a linear variation. The recovery of the enzyme activity was expressed by

$$E_N = \sum_{i=1}^{n} E_i(1 - e^{-k_i t})$$

with $\sum_{i=1}^{n} E_i = E_0$, E_0 being the total enzyme concentration. The enzyme activity under steady-state conditions was given by

$$-dA/dt = k_{cat} E_N$$

A being the absorbance of the product. The resolution of these equations gave

$$A = A_0 + \sum_{i=1}^{n} A_i e^{-k_i t} + ct$$

with

$$A_i = k_{cat} E_i / k_i \qquad c = \sum_{i=1}^{n} A_i k_i$$

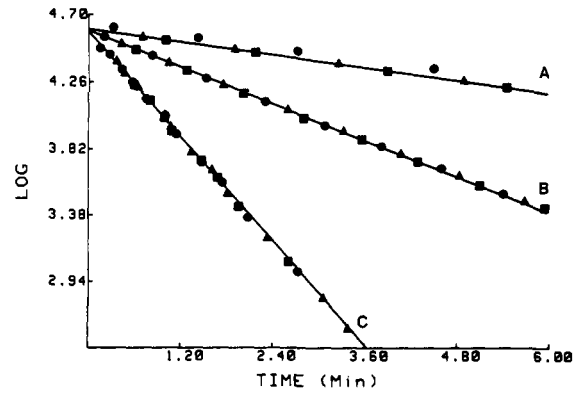

FIGURE 1: Semilog plot of unfolding kinetics followed by tryptophan fluorescence (■), circular dichroism at 220 nm (●), and enzyme activity (▲) for different final Gdn-HCl concentrations: 0.8 (A), 1 (B), and 1.4 M (C). Initial conditions: 80 μM PGK in 100 mM phosphate buffer, pH 7.5; final concentration of PGK 2 μM. The experiments were carried out at 23 °C.

Experimental curves were analyzed by a multilinear regression program with an iterative search of the parameters with the help of a Hewlett-Packard 9816 calculator.

Simulations of the Kinetics. Simulations of the experimental kinetics were realized by numeric integration of differential equations derived from several plausible models and by using the method of Kûbicek & Vishnak (1974), coupled with the simplex procedure (Nedler & Mead, 1965) (see Appendix).

Results

Kinetics of Unfolding. (A) Kinetics Followed by Fluorescence and by Circular Dichroism. Kinetics were followed by fluorescence emission at 336 nm and by variations in ellipticity at 220 nm, these two signals reflecting different characteristics of the protein structure. Nevertheless, in a concentration range of Gdn-HCl from 0.8 to 2 M for both signals, the denaturation kinetics were describable in a first approximation by only one exponential term (Figure 1). For higher concentrations of denaturant in the unfolded base-line region, the macroscopic rate constant increased with the concentration of denaturant; a stopped-flow method was therefore required to follow the kinetics. Even under these conditions, monophasic kinetics were observed. The first-order macroscopic rate constant was not depending on the concentration of protein (between 0.5 and 5 μM).

For denaturant concentrations smaller than 0.8 M, it was difficult to follow the unfolding kinetics since the process was very slow and the amplitude was very small. However, we noted a small lag of about 1–2 min, but it was very difficult to analyze.

The normalized amplitudes extrapolated to $t \rightarrow \infty$ were superimposable to the corresponding transition curves (Figure 2) as expected from a monophasic folding process. Monotoneous variation of λ vs. Gdn-HCl concentration was observed whatever was the observable, suggesting that the modification in the ordered structure and the variations in the environment of tryptophans followed the same apparent kinetics.

(B) Kinetics Followed by the Loss of the Enzyme Activity. The enzyme activity was measured by a coupled assay as described under Materials and Methods. Therefore, it was not possible to record directly the kinetics of unfolding, and a stepwise procedure was used. Previously, it was checked that the residual concentration of Gdn-HCl inhibited the enzyme activity of neither PGK nor GPDH. As pointed out under Materials and Methods, the rate of reactivation must be the

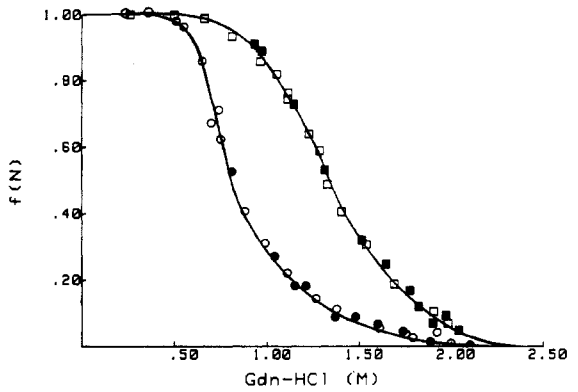

FIGURE 2: Plots of normalized amplitude for unfolding and refolding kinetics as a function of Gdn-HCl concentration: (circles) kinetics followed by circular dichroism; (squares) kinetics followed by fluorescence. Filled symbols represent the amplitude of the single phase obtained from unfolding kinetic experiments. Open symbols represent the total amplitude ($A_1 + A_2$) obtained from refolding kinetic experiments. Full lines referred to the transition obtained from equilibrium data (Betton et al., 1984).

rate-limiting step. These conditions were verified for concentrations of Gdn-HCl smaller than 0.06 M and concentrations of PGK in the denaturant higher than 0.1 μM. It was not possible to follow the kinetics of inactivation for Gdn-HCl concentrations higher than 1.5 M, the process becoming too fast. As illustrated in Figure 1, the unfolding kinetics followed by the loss of enzyme activity were also monophasic; furthermore, the macroscopic rate constant was found identical with that determined from optical signals for each concentration of denaturant. Thus, by three different methods the same kinetics of unfolding were recorded, describable in a first approximation by only one exponential term.

Kinetics of Refolding. Kinetics of refolding were recorded under experimental conditions identical with those used for the unfolding process (pH, temperature, and final concentration of protein). Under these conditions, biphasic kinetics were observed by fluorescence and by circular dichroism, describable by

$$A(t) = A_1 e^{-\lambda_1 t} + A_2 e^{-\lambda_2 t}$$

Two ranges of Gdn-HCl concentrations were characterized by differences in the sign of the amplitudes (Figure 3). Between 2 and 0.75 M Gdn-HCl, both phases had a negative amplitude in fluorescence experiments, and the amplitude of the slower phase (A_2) was zero in the kinetics followed by circular dichroism.

Between 0.7 and 0.06 M Gdn-HCl, in fluorescence experiments, the fast phase had a negative amplitude (A_1) reaching 150% of the total variation, and the slower phase had a positive amplitude (A_2). Both phases had a negative amplitude when the kinetics were followed by circular dichroism.

Analysis of the Fast Phase. This phase was only detected for the refolding process. It was too fast to be analyzed by manual mixing. Indeed, it was even faster than the dead time of a stopped-flow machine (5 ms) equipped with fluorescence detection. Thus, the values of λ_1 could not be determined.

We obtained informations only about the amplitudes (Figure 4). The amplitude A_1 values observed by both fluorescence emission and circular dichroism were negative. For fluorescence, this negative amplitude reached a value higher than the total amplitude, corresponding to complete refolding. Such an increase of the amplitude up to 1.5 was not observed on the ellipticity at 220 nm. For this signal, the optimal value of the amplitude extrapolated to a concentration of Gdn-HCl equal to zero was 0.55.

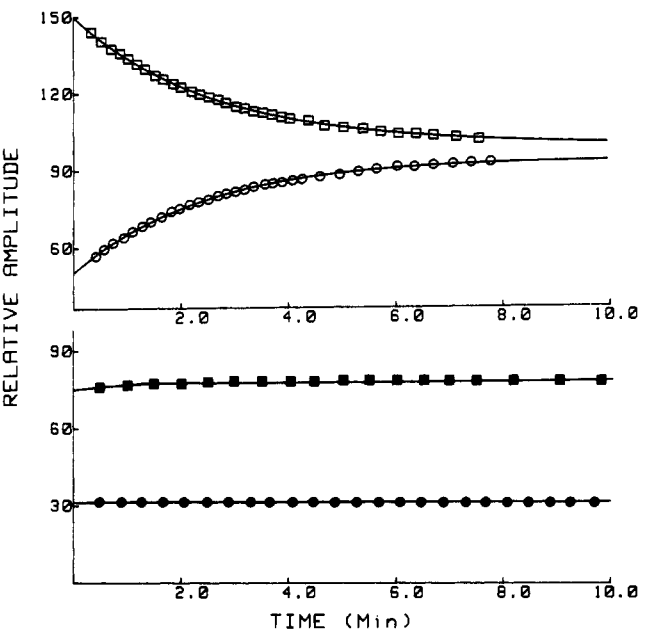

FIGURE 3: Refolding kinetics followed by fluorescence emission at 336 nm (squares) and by circular dichroism at 220 nm (circles). Initial conditions: PGK (8 μM) in 100 mM phosphate buffer containing 6 M Gdn-HCl, pH 7.5. Final conditions: PGK (2 μM) in 100 mM phosphate buffer, pH 7.5, containing 0.2 M Gdn-HCl (open symbols) or 1 M Gdn-HCl (closed symbols). Data points obtained from continuous recording.

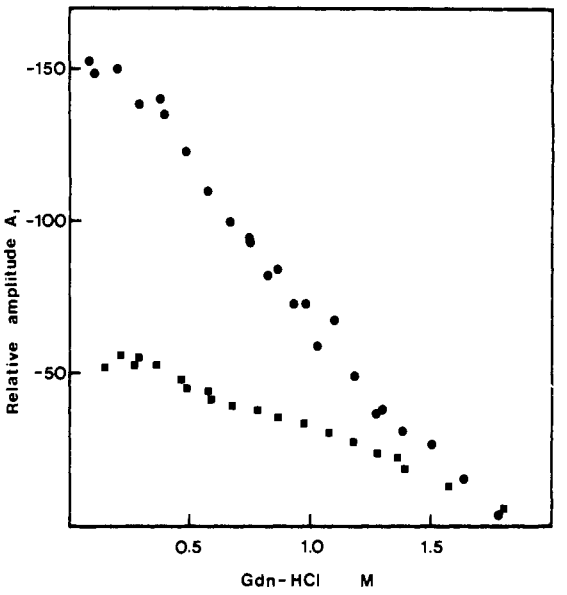

FIGURE 4: Plots of normalized amplitude for the fast refolding phase (A_1) as a function of final Gdn-HCl concentration. Closed circles represent A_1 obtained from fluorescence measurements extrapolated at zero time. Closed squares represent A_1 obtained from circular dichroism measurements extrapolated to zero time.

Analysis of the Slow Phase. The slow phase that followed had, however, a positive amplitude (see below). Figure 5 indicates the variations in λ_2 with the concentration of denaturant for both signals (fluorescence and ellipticity at 220 nm) determined during the unfolding and the refolding processes. In the range of Gdn-HCl concentration between 0.7 and 2 M, the same identical variations in λ were observed for denaturation and renaturation, i.e., independently of the initial conditions. A discontinuity in the curve log λ vs. denaturant concentration was noted for 0.7 M Gdn-HCl, which is about the critical concentration for which an apparent irreversibility

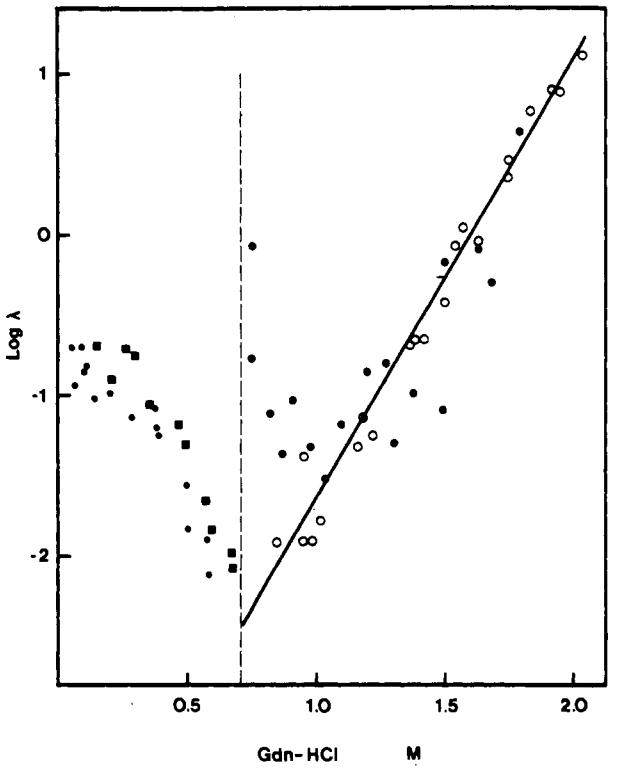

FIGURE 5: Plots of macroscopic rate constant (λ_2) for the refolding phase as a function of final Gdn-HCl concentration: (closed circles) fluorescence measurements; (closed squares) circular dichroism measurements. Open circles represent the macroscopic rate constant obtained from unfolding kinetics. Dashed line represents an hypothetic asymptote for 0.7 M Gdn-HCl.

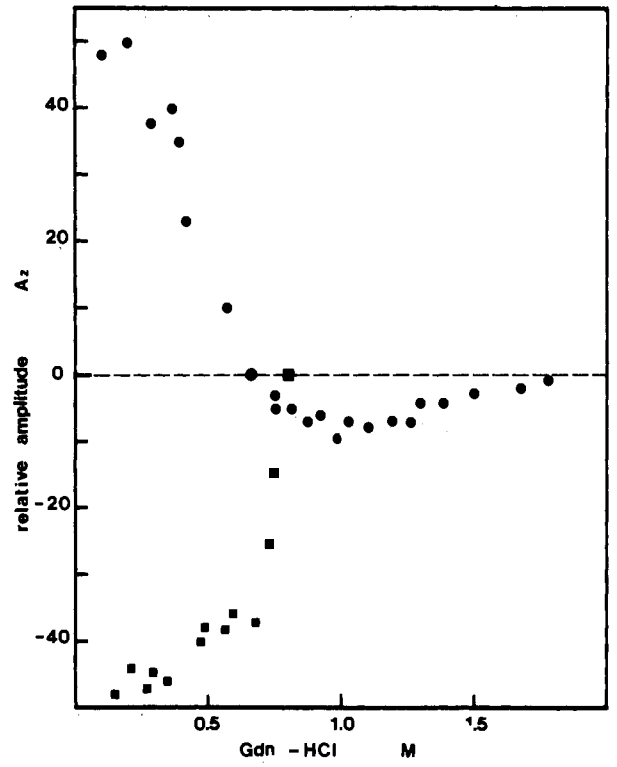

FIGURE 6: Plots of normalized amplitude for the slow refolding phase (A_2) as a function of final Gdn-HCl concentration. Closed circles represent A_2 obtained from fluorescence measurements. Closed squares represent A_2 obtained from circular dichroism measurements.

was observed. In the range between 0 and 0.7 M Gdn-HCl concentration, the same λ values were obtained for both signals. Figure 6 indicates the variation in amplitude for the slow phase of refolding, observed by fluorescence and by circular dichroism. The maximum variation in amplitude associated with this slow phase was around 0.45–0.5 for both signals.

Both signals led to the detection of the same slow phase. It is likely that this phase reflected structural changes involving the same part of the molecule in which both the environment of tryptophan and the ordered structures were modified.

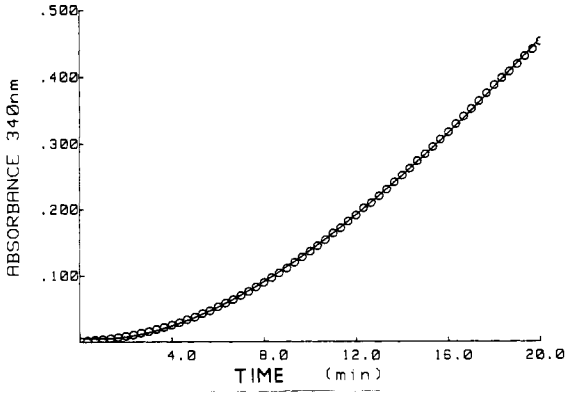

FIGURE 7: Reactivation kinetics followed by direct recording. Kinetics were followed by the appearance of NADH at 340 nm and analyzed with the equation $A = A_0 + A_r e^{-\lambda_r t} + Ct$ (see text). Data points were obtained from continuous recording.

Kinetics of Recovery of the Enzyme Activity. As mentioned under Materials and Methods, the kinetics of reactivation were not directly recorded. We studied only the kinetics of total reactivation of an enzyme previously denatured in 6 M Gdn-HCl and then diluted to 0.06 M Gdn-HCl. Figure 7 shows a recording of the kinetics fitted according to

$$A = A_0 + A_r e^{-\lambda_r t} + Ct$$

A being the absorbance of NADH at 340 nm in the coupled enzyme assay.

The rate constant thus obtained was slightly smaller than the slower rate constant determined from variations in optical signals ($\lambda = 0.1$ min^{-1} at 23 °C). The enzyme activity was nil at zero time, indicating that the fast phase of refolding as detected from the optical signals reflected an inactive intermediate. Furthermore, the rate constant observed when the steady state was reached corresponded only to 7% of that observed with the native enzyme under the same conditions (1 μM PGK), whereas 85% was expected. Such a situation suggested a possible equilibrium between two denatured forms of the enzyme. Similar results obtained for RNase A (Garel & Baldwin, 1973) was earlier explained by an isomerization of prolines although the step where this isomerization took place remained unclear. PGK contains 13 prolines, 2 of which are in the cis form in the native protein. With the aim to investigate the plausibility of the proline isomerization as the slower step in the refolding of PGK, double-jump experiments similar to those described by Brandts et al. (1975) were performed. We incubated the protein for various periods in 6 M Gdn-HCl, and we studied the reactivation kinetics as a function of the time of incubation in 6 M Gdn-HCl. Neither the apparent macroscopic rate constant nor the amplitude of reactivation was found to depend on the time of incubation. This discarded the possible existence of two denatured forms in equilibrium. In the study of the transition curve at equilibrium, 85% yield was reached for reactivation (Betton et al., 1984). But the conditions of regeneration were different. For the refolding under equilibrium conditions, the denatured protein was incubated in the regeneration mixture devoid of ligands. To study the kinetics of refolding, reactivation was

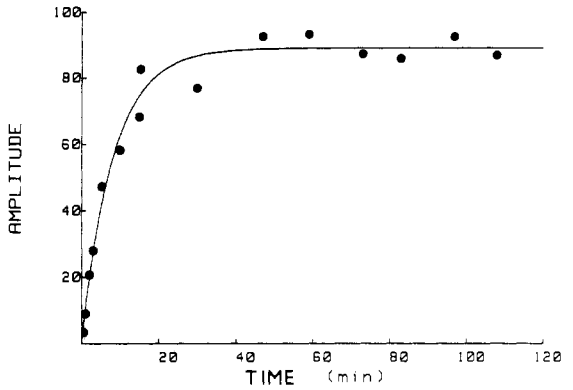

FIGURE 8: Reactivation kinetics at 23 °C, pH 7.5. PGK was denatured for 24 h in 6 M Gdn-HCl and then diluted (1/100) into the regeneration buffer prior to measuring the enzyme activity.

performed in the presence of specific substrates. It was observed (A. Mitraki et al., unpublished data) that ligands were able to bind an intermediate and to prevent the correct folding of the protein. Thus, in another set of experiments, when the renaturation was made to occur in the absence of ligands (Figure 8), we found the expected value for both the reactivation yield and macroscopic rate constant (0.15 min^{-1}).

Analysis of the Data. Equilibrium studies clearly indicated the existence of at least one intermediate. The studies on the reversibility of the unfolding process showed that one or more intermediates can be stabilized under critical concentration of denaturant. Kinetic studies revealed at least two phases. Furthermore, the fast phase observed by fluorescence had a normalized amplitude higher than 1 (1.5); this prevented the use of classical diagnostic rules, since neither those developed by Ikai & Tanford (1973) nor those derived by Hagerman (1977) apply under these conditions.

To analyze the data, first we determined the fluorescence emission spectrum of the intermediate responsible for the amplitude higher than that of the native protein. Second, kinetics corresponding to different schemes of folding pathway were simulated. Since we had only a little information on the fast reaction, for the sake of simplicity we assumed it to be monophasic. The results obtained from simulation were compared with the experimental data.

(A) Determination of the Emission Fluorescence Spectrum of the Intermediate. To determine the fluorescence emission spectrum of the intermediate, refolding kinetics were followed at various emission wavelengths (excitation 292 nm), and the amplitude of the slow phase was extrapolated to $t = 0$ for each wavelength by fitting to the relationship

$$y = A_1 + A_2 e^{-\lambda_2 t}$$

Figure 9 shows the emission spectra of the native protein and that of the intermediate X thus obtained. The spectrum of the intermediate indicated both a blue shift and an hyperchromicity compared with that of the native protein, suggesting that tryptophans were in a more apolar environment than in the native protein.

(B) Analysis of the Data Using Simulation of the Kinetics. Since the λ values were identical for the forward and reverse reactions, kinetics could be described by a phenomenological equation consisting of the sum of two exponential terms:

$$y = A_1 e^{-\lambda_1 t} + A_2 e^{-\lambda_2 t}$$

Different schemes, able to account for biphasic kinetics, were

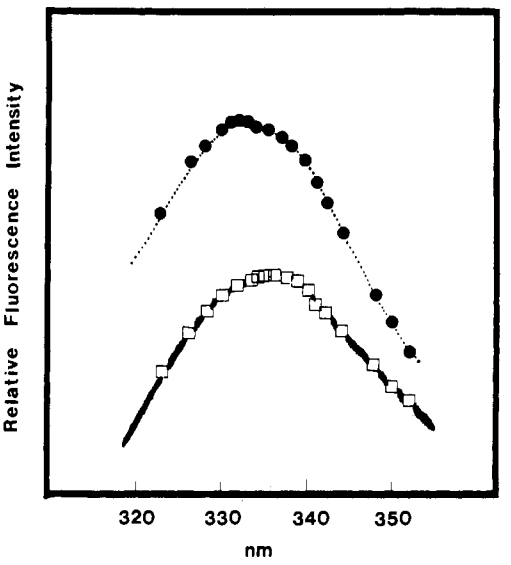

FIGURE 9: Fluorescence emission spectrum of the intermediate accumulated during the fast phase of refolding (PGK denatured in 4 M Gdn-HCl was diluted at $t = 0$ in the regeneration buffer, to a final concentration of 1 μM). λ_{exc} = 292 nm. (□) Fluorescence intensity at $t \rightarrow \infty$; (●) fluorescence intensity extrapolated to zero time of the slow phase; (heavy line) emission spectrum of native PGK in the same conditions.

examined and the kinetic behavior was generated by simulation. The following models were studied:

$$N \underset{k_2}{\overset{k_1}{\rightleftharpoons}} X \underset{k_4}{\overset{k_3}{\rightleftharpoons}} D \quad (1)$$

$$N \underset{k_2}{\overset{k_1}{\rightleftharpoons}} D \underset{K_4}{\overset{k_3}{\rightleftharpoons}} X \quad (2)$$

$$X \underset{k_2}{\overset{k_1}{\rightleftharpoons}} N \underset{k_4}{\overset{k_3}{\rightleftharpoons}} D \quad (3)$$

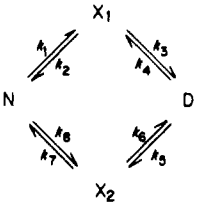

(4)

Although the classical diagnostic rules did not apply, we could discard some of these models from simple criteria.

Since there was a fluorescence burst of 150%, we can attribute a normalized coefficient of at least 1.5 to the intermediate. Similarly, a burst of 50% was observed when renaturation kinetics were followed by ellipticity recording at 220 nm. Assuming only one species responsible of this burst, an ellipticity coefficient of 0.5 was attributed to the same intermediate. Furthermore, this intermediate species had no enzyme activity. Therefore, models 2 and 3 could not account for these data.

Examination of models 1 and 4 required simulations. For both models we had the following relationship:

$$y = r_N f_N + r_D f_D + r_i f_i$$

y being the observed signal (fluorescence, ellipticity, or enzyme activity), as a function of time, r_N, r_D, and r_i being the normalized fractions of the signal characteristic of native, denatured, and intermediate species, respectively, and f_N, f_D, and f_i being the corresponding fractions of these species with the relation

$$f_N + f_D + f_i = 1$$

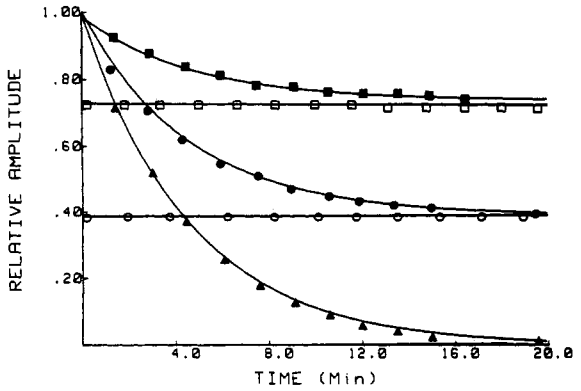

FIGURE 10: Simulated kinetics of the unfolding and refolding of PGK according to model 1 in 1 M Gdn-HCl final concentration. The points reported in the curve were obtained by circular dichroism (●, ○), fluorescence (■, □), and enzyme activity (▲). Closed symbols referred to the unfolding process; open symbols, to the refolding.

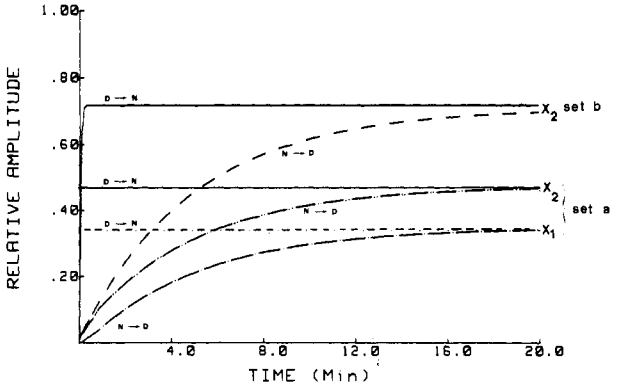

FIGURE 11: Simulated kinetics of the formation of intermediates X_1 and X_2 according to model 4, during the unfolding (N → D) and the refolding (D → N) of PGK, using the two sets of parameters as indicated in the text.

For simulation of model 1, we used the following parameters: for fluorescence, $r_N = 1$, $r_X = 1.5$, and $r_D = 0$; for ellipticity, $r_N = 1$, $r_X = 0.5$, and $r_D = 0$; for enzyme activity, $r_N = 1$ and $r_X = r_D = 0$. For simulation of model 4, two sets of values were tested for fluorescence, either (a) $r_N = 1$, $r_{X_1} = 1.5$, and $r_{X_2} = 1$ or (b) $r_N = 1$, $r_{X_1} = 0.5$, and $r_{X_2} = 0.5$; for circular dichroism we used only $r_N = 1$, $r_{X_1} = 0.5$, and $r_{X_2} = 0.5$ and for enzyme activity $r_N = 1$ and $r_{X_1} = r_{X_2} = r_D = 0$. For all signals, $r_D = 0$.

Simulations were performed according to the procedure described in the Appendix for several values of final concentrations of Gdn-HCl along the transition curve.

For model 1, monophasic kinetics with a positive amplitude were expected only for $k_1 \ll k_3$ for the unfolding process. When this condition was not fulfilled, the model predicted biphasic kinetics. Computations with several values of the k_1/k_3 ratio allowed us to find conditions where a lag would be observable.

For the refolding process, $k_4 \gg k_2$, since the first step was very fast. However, the indetermination on the λ_1 experimental values prevented any comparison between simulated and experimental kinetics. Since the fast phase was not observable, even by stopped flow, it was assumed that λ_1 is larger than 10^4 min^{-1}.

Simulated kinetics under final conditions of complete unfolding and refolding had the same characteristics as the experimental ones for adequate values of k_{ij}. Simulated kinetics for final concentrations of denaturant in the unfolded and folded base-line range and also in the transition region that was more significant were consistent with the experimental data obtained by the different methods. Figure 10 illustrates such kinetics for the unfolding and the refolding of PGK in 1 M Gdn-HCl final concentration. However, several restrictions have to be mentioned. During simulation, it was not possible to find conditions able to account quantitatively for variations of λ_2, the macroscopic rate constant of the slow phase of renaturation.

Furthermore, the study of the dependence of microscopic rate constants vs. the concentration of denaturant showed that k_2 did not vary monotoneously with Gdn-HCl concentration but displayed sigmoidal variations; such variations did not seem plausible and suggested that model 1 was too oversimplified to describe the folding pathway of horse muscle PGK.

For model 4, simulated curves were also calculated for several Gdn-HCl concentrations in the transition region and in the unfolded and folded base-line range. We obtained simulated kinetics that agreed with the experimental data as well for parameters a as for parameters b. The same profiles as those in Figure 10 were obtained. Figure 11 illustrates the variations of the species vs. time for the two sets of fluorescence parameters in 1 M Gdn-HCl.

Discussion

In a previous work (Betton et al., 1984), the data obtained from equilibrium measurements showed the occurrence of intermediates in the Gdn-HCl-induced reversible transition of horse muscle PGK. Kinetic studies were performed in order to determine the number of intermediates and to obtain information on the folding pathway. For the refolding process, biphasic kinetics were observed, whatever was the observable; only the slow phase was detected for the unfolding process.

The slow phase was not attributable to proline isomerization, since (1) it depended on the denaturant concentration and (2) the reactivation kinetics were not depending on the time of incubation in 6 M Gdn-HCl. Furthermore, the intermediate had neither the properties of the denatured nore those of the native protein. Working at several wavelengths, it was possible to obtain the fluorescence emission spectrum of the intermediate in which tryptophan seemed more buried than in the native protein. These species had about 50% ordered structures and no enzyme activity. Kinetic analysis indicated that these species were located between the native and the denatured protein.

The two simplest schemes able to account for biphasic kinetics were analyzed. Although the best fit was obtained with model 4, model 1 cannot be completely discarded from kinetic studies presented in this paper. But comparison of these data with previous results obtained by our group (Betton et al., 1984; A. Mitraki et al., unpublished data) indicating a partial irreversibility of the reactivation process under critical concentration of denaturant (0.8 M Gdn-HCl) provides additional arguments to discard model 1. The existence of a "trough" for 0.8 M Gdn-HCl would necessitate modifying model 1 by the following:

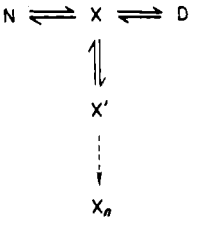

X′ being a partially and incorrectly folded species and X_n being aggregates. In such a model with only one intermediate in the folding pathway, the coefficient r_X for fluorescence must

be taken equal to 1.5 according to the experimental data. Thus, during refolding kinetics at low denaturant concentration, followed by fluorescence, a burst must be expected. This was predicted by simulation of the kinetics at 0.8 M Gdn-HCl but never observed experimentally.

Model 4 could be modified to take account of the additional data related to the partial irreversibility of reactivation observed at 0.8 M Gdn-HCl, as follows:

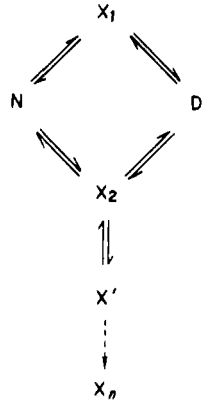

And, it could be analyzed with the two sets of fluorescence parameters (a and b, see above). When r_{X_2} was taken equal to 0.5, the ratio X_1/X_2 was 0.3 at 0.8 M Gdn-HCl and very close to 1 for denaturant concentrations larger than 1 M. When r_{X_2} was taken equal to 1 for Gdn-HCl concentrations equal or larger than 0.8 M, X_1/X_2 was very small, and only X_2 species were significantly populated for Gdn-HCl concentrations smaller than 0.8 M. For denaturant concentrations larger than 0.8 M, the reaction followed preferentially $N \rightarrow X_2 \rightarrow D$. For denaturant concentrations smaller than 0.8 M, the pathway $N \rightarrow X_1 \rightarrow D$ was preferred (as observed in the refolding process). Furthermore, at 0.8 M Gdn-HCl (according to parameters b), the intermediate that accumulated had a fluorescence coefficient $r_{X_2} = 1$, and no burst was obtained by simulation of the kinetics, in agreement with the experimental data since a burst in fluorescence was only observed for Gdn-HCl concentrations smaller than 0.7 M. Thus, it seems likely that the intermediate X_3 has a fluorescence coefficient closer to 1 than to 0.5. In this scheme, the fluorescence spectrum of the intermediate observed during the refolding process is related to the X_1 species.

Such a model is the simplest plausible one accounting for most of the data obtained until now. We have no information about the very fast phase of refolding. For the sake of simplicity, we assumed it was a single step. Other experiments under way in our laboratory in the presence of specific ligands might provide further informations on the folding pathway of horse muscle PGK.

ACKNOWLEDGMENTS

We thank Dr. Ghélis, Dr. Goldberg, Dr. Janin, Dr. Karplus, Dr. Perahia, and Dr. Colonna for very helpful discussions and suggestions. We are indebted to Dr. Banerjee for carefully reading the manuscript and Dr. Guschlbauer for the use of his dichrograph.

APPENDIX

In many cases the analysis of chemical schemes leads to differential equation systems difficult to resolve. Several integration techniques were developed; among them, the algorithm proposed by Kubicek & Visnack (1974) used in this study shows several advantages. It is efficient for any kind of scheme, whether cyclic or not, even when the microscopic constants that define the model have very different values (stiff model). Moreover, it is useful even when some steps involve more than one species.

This method leads to a linear equation, which integrates the differential equation system

$$y_i = f_i(x, y_1, y_2, y_3, ..., y_n)$$

with the initial conditions $y_i c$ by using an integration step, h. At each step k, y_i^{c+kh} is computed with an integration step h and $h/2$. When the error between the two computations is inferior to the allowed tolerance, the values y_i^{c+kh} are used as new initial conditions, and the process continues. Otherwise, a next integration step is computed. With such an algorithm, the integration requires only writing the differential equations and the corresponding elements of the Jacobian matrix.

The differential equations associated with model 1 were

$$dX/dt = k_1N - (k_2 + k_3)X + k_4D$$

$$dD/dt = k_3X - k_4D$$

and those associated with model 4 were

$$dX_1/dt = k_1N - (k_2 + k_3)X_1 + k_4D$$

$$dX_2/dt = k_3N - (k_1 + k_4)X_2 + k_2D$$

$$dD/dt = k_3X_1 + k_1X_2 - (k_4 + k_2)D$$

With a set P of microscopic constants $p_1, p_2, p_3, ..., p_n$, we obtain the vector y for each step. The amplitude of the signal at the integration step $c + hk$ is

$$S_p^{c+kh} = \sum_{i=1}^{n} r_i y_i^{c+kh}$$

where r_i is the weighting factor related to the species y_i. To obtain the representative simulated curve with the best fit of the experimental points, we had to minimize the value:

$$\Delta = \sum_{hk=0}^{t} (S_p^{c+kh} - S_{exp}^{c+kh})^2$$

t being the integration time and S_{exp}^{c+kh} the experiment value of the signal at time $c + kh$.

Since there is no explicit relation between S^{c+kh} and the vector P cannot be minimized according to the classical methods, such as least-squares regression, steepest descent, or other related methods, to minimize we developed an algorithm derived from the method of Nelder & Mead (1965). This method is strictly convergent and can be used to minimize any kind of function, even when partial derivatives are not possible to determine, as in the present case.

Since the procedure developed by Kubicek and Visnak allows an automatic change of the integration step, the function Δ was weighted by the value h. Thus, the following function was minimized:

$$\Delta = \sum_{kh=0}^{t} h(S_p^{c+kh} - S_{exp}^{c+kh})^2$$

with the condition $\sum kh$ = constant for all sets of parameters P.

Registry No. PGK, 9001-83-6; Gdn-HCl, 50-01-1.

REFERENCES

Baldwin, R. L. (1975) *Annu. Rev. Biochem. 891*, 453–475.

Banks, R. D., Blake, C. C. F., Evans, P. R., Haser, R., Rice, D. W., Hardy, G. W., Merrett, M., & Phillips, A. W. (1979) *Nature (London) 279*, 773–777.

Betton, J. M., Desmadril, M., Mitraki, A., & Yon, J. M. (1984) *Biochemistry 23*, 6654–6661.

Blake, C. C. F., & Rice, D. W. (1981) *Philos. Trans. R. Soc. London 293*, 93–104.
Blake, C. C. F., Evans, P. R., & Scopes, R. K. (1972) *Nature (London) 235*, 195–198.
Brandts, J. F., Halvorson, H. R., & Brennan, M. (1975) *Biochemistry 14*, 4953–4963.
Bucher, T. (1955) *Methods Enzymol. 1*, 415–422.
Cleland, W. W. (1967) *Adv. Enzymol. Relat. Areas Mol. Biol. 29*, 1–32.
Desmadril, M., Mitraki, A., Betton, J. M., & Yon, J. M. (1984) *Biochem. Biophys. Res. Commun. 118*, 416–422.
Garel, J. R., & Baldwin, R. L. (1973) *Proc. Natl. Acad. Sci. U.S.A. 70*, 3347–3351.
Ghelis, C., & Yon, J. M. (1982) *Protein Folding*, Academic Press, New York.
Hagerman, P. J. (1977) *Biopolymers 16*, 731–747.
Ikai, A., & Tanford, C. (1973) *J. Mol. Biol. 73*, 145–163.
Jaenicke, R., & Rudolph, R. (1980) in *Protein Folding* (Jaenicke, R., Ed.) pp 525–548, Elsevier/North-Holland, Amsterdam.
Kim, P. S., & Baldwin, R. L. (1982) *Annu. Rev. Biochem. 51*, 459–489.
Kubicek, M., & Vishnak, K. (1974) *Chem. Eng. Commun. 1*, 291–296.
Nelder, J. A., & Mead, R. (1965) *Comput. J. 7*, 308.
Nozaki, Y. (1970) *Methods Enzymol. 26*, 43–50.
Rudolph, R., Zettlmeissl, G., & Jaenicke, R. (1979) *Biochemistry 18*, 5572–5575.
Schmid, F. X. (1983) *Biochemistry 22*, 4690–4696.
Scopes, R. K. (1969) *Biochem. J. 113*, 551–554.

Association–Dissociation Equilibria of *Octopus* Hemocyanin†

K. E. van Holde and Karen I. Miller*
Department of Biochemistry and Biophysics, Oregon State University, Corvallis, Oregon 97331
Received December 26, 1984

ABSTRACT: The equilibria between the native (decameric) *Octopus* hemocyanin and its subunits were studied by analytical sedimentation. Equilibrium is obtained slowly, but the reaction is thermodynamically reversible. The mass action law for a monomer–decamer reaction is obeyed. The reassociated hemocyanin is virtually identical in its sedimentation behavior and oxygen binding with the native protein. The association–dissociation equilibria are mediated by cations; Mg^{2+}, Ca^{2+}, Na^{+}, and H^{+} are all effective in stabilizing the decameric form at appropriate concentrations. About three to four cations per monomer must be bound for association to occur. Under some conditions, dimers of the subunits can be observed, but formation of this dimer does not depend on cation concentration, and it does not appear to be an obligate intermediate in the association to decamer.

In a previous publication (Miller & van Holde, 1982), we have characterized the subunit structure of the hemocyanin from *Octopus dofleini*. In this paper, we shall describe studies of the association–dissociation equilibria of this protein.

The *Octopus* hemocyanin exists in the hemolymph as a 51S decamer of 11S subunits. Such decameric structures are common among the molluscan hemocyanins (van Holde & Miller, 1982; Ellerton et al., 1983). However, in cases investigated so far, attempts to reassociate the subunits to create decamers have not been quantitatively successful. For example, in his extensive studies of the *Helix pomatia* hemocyanin, Siezen (1974) found that 11S subunits reassociated very poorly, with the formation of numerous intermediate structures. Even with the relatively well-behaved *Loligo* hemocyanin, van Holde & Cohen (1964a) achieved no more than 75% reassociation. Similar results were obtained by Brouwer et al. (1978) with *Murex* hemocyanin. The reasons for these limitations are obscure but may relate to subunit heterogeneity (Siezen & van Driel, 1973; Brouwer et al., 1978). In any event, they signify that the dissociation of these hemocyanins is not wholly reversible, which invalidates most studies of its thermodynamics. This is unfortunate, for thermodynamic analysis of equilibria involving such large subunits and their aggregates would be of considerable general interest. Furthermore, fundamental studies of ligand binding are of uncertain validity if the thermodynamic state of the system is not well-defined.

Therefore, we were extremely pleased to note in the earlier studies that *Octopus dofleini* hemocyanin could be *quantitatively* reassociated from subunits by such simple treatments as the addition of divalent cations to the solution. This has prompted us to undertake a detailed study of the association states of this hemocyanin and the equilibria connecting these. This paper describes these experiments. The results provide a defined framework for the oxygen binding studies described in the following paper (Miller, 1985).

Materials and Methods

Preparation of the Hemocyanin Solutions. Hemolymph was taken from live, ethanol-anaesthesized octopi either by cannulation of the vena cava or by hypodermic extraction from the afferent branchial vein. The hemolymph was kept sterile and on ice for transportation to the laboratory, at which point it was centrifuged at low speed and 0.1% phenylmethanesulfonyl fluoride was added as a protease inhibitor. It was then stored at 4 °C; such samples appeared, from sedimentation studies, to be stable for at least 2 months.

For purification of the hemocyanin, the hemolymph was passed over an A5-M column, equilibrated with I = 0.1

†This work was supported by National Science Foundation Grant PCM82-12347.

0006-2960/85/0424-4577$01.50/0